THE JOURNAL OF PHYSICAL CHEMISTRY C

Article

pubs.acs.org/JPCC

Probing the Dynamics of the Porous Zr Terephthalate UiO-66 Framework Using ^{2}H NMR and Neutron Scattering

D. I. Kolokolov,[†,∥] A. G. Stepanov,[†] V. Guillerm,[‡] C. Serre,[‡] B. Frick,[§] and H. Jobic*[,∥]

[†]Boreskov Institute of Catalysis, Siberian Branch of Russian Academy of Sciences, Prospekt Akademika Lavrentieva 5, Novosibirsk 630090, Russia

[‡]Institut Lavoisier, UMR CNRS 8180, Université de Versailles Saint-Quentin-en-Yvelines, 78035 Versailles, France

[§]Institut Laue Langevin, BP 156, 38042 Grenoble, France

[∥]Institut de Recherches sur la Catalyse et l'Environnement de Lyon, UMR CNRS 5256, Université Lyon 1, 2. Av. A. Einstein, 69626 Villeurbanne, France

Supporting Information

ABSTRACT: ^{2}H NMR and quasi-elastic neutron scattering techniques have been used to study the rotational dynamics of the 1,4-benzene-dicarboxylate (BDC) linkers in the porous cubic UiO-66(Zr) metal−organic framework (MOF). The rotation of the benzene rings in the BDC linkers is at the limit of detection of the neutron technique, but it fits perfectly on the ^{2}H NMR time scale. The aromatic rings in the UiO-66 framework exhibit the lowest rotational barrier compared to other MOFs, the activation energy for π-flips being 30 kJ mol^{-1}. However, instead of having well-defined flipping rates like in MOF-5, MIL-47, or MIL-53, UiO-66(Zr) shows a distribution of flipping correlation times, probably due to local disorder in the structure. Because of the rotational motion of the benzene rings, the effective size of the microporous windows in UiO-66(Zr) appears to be temperature dependent.

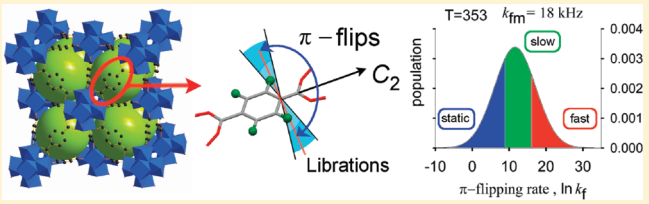

1. INTRODUCTION

The efficiency of a given microporous system, e.g., for separation processes, depends on the interaction mechanism between the adsorbed molecular species and the hosting material; i.e., it is a matter of interaction on the molecular scale. This interaction governs not only the thermodynamics of a given adsorption-based process but also its kinetics, the second fundamental parameter that can strongly affect the overall efficiency.

Metal−organic frameworks (MOFs) or porous coordination polymers (PCPs) represent a rapidly expanding family of novel nanoporous materials with potential applications in the fields of adsorption or separation of gases and liquids, catalysis, drug delivery, and others.[1−4] MOFs belong to a class of coordination polymers built from metal oxide nodes connected together by bridging organic "linkers" (carboxylates, azolates, phosphonates, etc.). The growing interest in these hybrid porous materials relies on their high surface area and accessible free pore volume as well as on their unique chemical versatility.[5] The latter is a remarkable feature, as the sorbent/sorbate interaction can be tuned by a proper choice of the metal center or of the organic linker, either through direct synthesis or postsynthesis modification, to meet the desired properties.[5,6] Some MOFs represent also a complex and intriguing type of regular porous system, as their framework is flexible and can expand or even "breathe"[7] upon adsorption, which additionally influences the guest molecules.

One of the key issues for MOFs is their hydrothermal stability.[8] In this respect, the recently synthesized MOF UiO-66(Zr)[9] has attracted particular interest. This zirconium-based microporous material is built from eight coordinated Zr polyhedra that assemble into $Zr_6O_4(OH)_4$ oxoclusters related together by 1,4-benzene-dicarboxylate (BDC) linkers. This results in an extended cubic porous system delimiting a 3D pore system composed of octahedral cages (free diameter ∼11 Å) surrounded in each corner by tetrahedral cages (free diameter ∼8 Å) interconnected by microporous triangular windows (free diameter ∼5−7 Å). UiO-66(Zr) exhibits a high surface area, a very good thermal stability, and interestingly an outstanding chemical stability (against water, acetone, dimethylformamide, and benzene).[9] Together with a relatively high working capacity, such properties make UiO-66 a promising material for a number of industrial processes like hexane and xylene isomer separation[10] or the separation of CO_2/CH_4 mixtures.[11] Currently, a considerable effort of the community is spent to modify the original structure with new linkers,[12−20] to tailor the framework for a number of specific applications.

The first investigations[11] on molecular diffusion in UiO-66(Zr) evidenced that the flexibility of the framework had to be

Received: March 27, 2012
Revised: May 14, 2012
Published: May 14, 2012

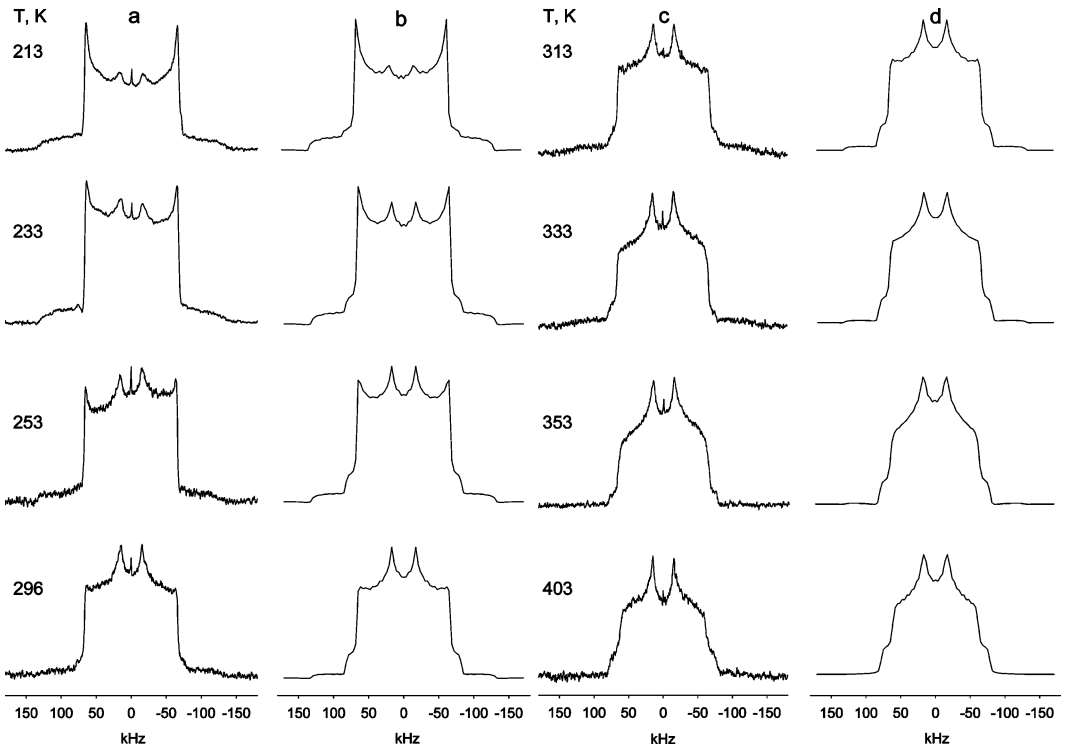

Figure 1. ^{2}H NMR temperature dependence of the spectral line shape for deuterated 1,4-benzene-dicarboxylate (BDC) linker fragments of UiO-66(Zr): experimental (a,c) and simulated (b,d) spectra.

taken into account during molecular dynamics (MD) simulations to correctly reproduce the experimental diffusivities. For molecules whose dimensions are comparable to the window size, the mobility of the benzene rings, acting as molecular rotors, should affect the effective size of the windows and thus the rate coefficients for cage-to-cage motions.

Furthermore, the mobility of the linkers in UiO-66 (as well as in any MOF) presents an interest in itself as it allows us to characterize the framework, leading to a better understanding of the structure on a microscopic level.[1,12,21−27] A detailed investigation of the UiO-66 structure has been carried out recently, showing a complete reversibility of the dehydration/hydration phenomenon and a distortion of the Zr_6O_6 units of the dehydrated material.[28,29] Here, we focus on the peculiarities of the benzene ring motions in the dehydroxylated form of UiO-66, by combining ^{2}H NMR spectroscopy and quasi-elastic neutron scattering (QENS) measurements.

2. EXPERIMENTAL SECTION

2.1. Materials. The synthesis and activation of UiO-66 was performed in accordance to the published procedures,[9] with deuterated or hydrogenated terephthalic acid as a reactant for the NMR or QENS experiments, respectively. The size of the crystallites is a few micrometers.

2.2. NMR Measurements. ^{2}H NMR experiments were performed at 61.424 MHz on a Bruker Avance-400 spectrometer using a high-power probe with a 5 mm horizontal solenoid coil. All ^{2}H NMR spectra were obtained by Fourier transformation of the quadrature-detected phase-cycled quadrupole echo arising in the pulse sequence ($90_x - \tau_1 - 90_y - \tau_2 -$ acquisition $- t$), where $\tau_1 = 20$ μs, $\tau_2 = 22$ μs, and t is a repetition time of the sequence during the accumulation of the NMR signal. The duration of the $\pi/2$ pulse was 1.8−2.3 μs. Spectra were typically obtained with 50 000 scans, and the repetition time was 1 s.

To capture all dynamical features of the system, the measurements were performed over a broad temperature range, from 143 to 403 K. The temperature of the samples was controlled with a variable-temperature unit BVT-3000 with a precision of ±1 K. The sample was allowed to equilibrate at least 15 min at a given temperature before the NMR signal was acquired.

To prepare the sample, 0.5 g of deuterated UiO-66 was loaded in a 5 mm (o.d.) glass tube, connected to a vacuum system. The sample was heated at 523 K for 12 h in air and for 24 h under a vacuum of 10^{-3} Pa. After cooling back to room temperature, the dehydroxylated form of the UiO-66 sample was sealed.

2.3. Neutron Measurements. The neutron experiments were performed on the backscattering spectrometer IN16, at the Institut Laue-Langevin, Grenoble. The incident neutron energy was 2.08 meV (6.271 Å), using a Si(111) monochromator. Spectra were recorded at different scattering angles, corresponding to wavevector transfers, Q, ranging from 0.19 to 1.9 Å^{-1}. Two acquisition modes were used: elastic and quasi-elastic scans. Quasi-elastic spectra were obtained by applying a Doppler shift to the incident neutrons through a movement of the monochromator. The energy transfer was then analyzed in a window of ±14.5 μeV, and the energy resolution was Gaussian like, with a fwhm < 1 μeV. In the other acquisition mode, the incident energy was kept constant so that only neutrons which were elastically scattered within the narrow energy resolution window of the spectrometer were detected. For this elastic scan, we used a counting time of 3 min per temperature step, ramping the sample temperature with 1.9 K/min below 80 and 0.48 K/min above.

dx.doi.org/10.1021/jp3029193 | J. Phys. Chem. C 2012, 116, 12131−12136

Hydrogenated UiO-66 was used for the neutron experiment. After activation at 523 K under vacuum (10^{-3} Pa), the sample was transferred inside a glovebox into a cylindrical aluminum container of annular geometry. The container was placed in a cryofurnace, so that measurements could be made in the temperature range 2−520 K.

3. RESULTS

3.1. ^{2}H NMR. Rotational dynamics of the UiO-66 organic linkers was probed by ^{2}H NMR over a temperature range 143−403 K. Experimental results, given in Figure 1 a,c, evidence that at 213 K and below the line shape is characterized by the Pake-powder pattern with Q_0 = 178 kHz and $\eta \sim 0$, characteristic of a static benzene ring on the ^{2}H NMR time scale ($\tau \gg \tau_Q$, $\tau_Q \sim Q_0^{-1} \sim 6 \times 10^{-6}$ s). Above 213 K, the line shape begins to evolve, presenting two symmetric peaks in the central part of the static spectrum. The further temperature evolution indicates an increasing mobility of the UiO-66 aromatic rings. The spectrum takes its final shape above 353 K, with an asymmetry parameter $\eta \sim 0.8$, i.e., a line shape typical of fast π-flips around a C_2 symmetry axis.

Within the UiO-66 structure, the benzene ring in the BDC linker has access to a limited number of motions. They correspond to: π-flips around the C_2 symmetry axis, librational motion in the potential well about the stable position, or a combination of both.

The first motion yields a very characteristic pattern, experimentally observed above 353 K. The uniaxial libration on other hand, when the libration angle is less than 20°, does not strongly change the line shape pattern but decreases the effective interaction constant Q.

A simple analysis of the spectra line shape indicates that at 403 K the spectrum is characterized by an effective interaction constant $Q \sim 80$ kHz, which is more than 10% smaller than the value expected for pure 2-fold uniaxial flips. A more refined approach with a model that takes into account both π-flips and the libration motion with an amplitude of 15° gives a very good fit of the experimental spectrum (see Figure 1d). Both motions are assumed to be in the fast exchange regime.

Such a finding indicates that by changing the flipping rate and the libration angle it should be possible to correctly fit the experimental spectra in the intermediate temperature range, where the spectrum is still not in the fast exchange limit. However, simulations according to such a model give no reasonable results. A detailed examination of the spectra in the intermediate temperature range reveals that, below 353 K, the spectrum shows a coexistence of the signal from static rings and from mobile rings. This case is well-known for solid polymer materials, and it indicates that instead of having well-defined flipping rates the organic linker dynamics is characterized by a distribution of flipping correlation times.

To describe this situation, we built a model that takes into account π-flips superimposed by small-angle librations characterized by a flipping correlation time disorder (see Supporting Information). The latter was found to be quite broad, so following previous works,[30,31] a log-normal distribution of the correlation times for the flipping motion was implemented.

This model depends on a reasonably limited number of fitting parameters: the mean value of the flipping correlation time $\tau_{fm} = k_{fm}^{-1}$ (where k_{fm} is the mean flipping rate constant), the width of the log-normal distribution σ, and the libration amplitude $\Delta\varphi/2$. Additional simulations showed that the librational motion can be considered to be fast at all temperatures. The simulation results in the intermediate temperature range (see Figure 1b,d) show that such a model describes quite well the experimental spectra. The fitting parameters are presented in Table 1.

Table 1. ^{2}H NMR Simulation Results: The First Columns Give the Line Shape Fitting Parameters for Each Studied Temperature. and the Last Three Columns Show the Population Evolution for Each Dynamical Range, i.e., for Static, Slow, and Fastly Reorienting Flipping Fragments[a,b]

	π-flip kinetics		libration amplitudes[c]	population factors		
T, K	k_{fm}, kHz	σ	$\Delta\varphi/2$	"static" $k_f < 10^3$, Hz	"slow flips" $10^3 < k_f < 10^6$, Hz	"fast flips" $10^6 < k_f$, Hz
213	15	5.0	<5°	0.295	0.506	0.199
233	110	5.1	<5°	0.178	0.491	0.331
253	400	5.2	<5°	0.125	0.448	0.427
296	2300	5.4	<5°	0.076	0.365	0.559
313	3300	5.5	<5°	0.071	0.343	0.586
333	12000	5.6	8°	0.047	0.283	0.669
353	18000	5.6	12°	0.040	0.263	0.696
403	60000	5.6	15°	0.025	0.209	0.766

[a] k_f is the actual flipping rate constant for a given aromatic ring; k_{fm} is the mean flipping rate; σ is the rate distribution width; and $\Delta\varphi/2$ is the libration angle amplitude. [b] The estimated errors are: ±10% for k_{fm}; ±0.1 for σ; ±10% for $\Delta\varphi/2$ (for $T \geq 333$ K). [c] The libration process is assumed to be rapid, being thus in the fast exchange limit, i.e., with $k_{lib} > 10^6$ Hz.

The temperature dependence of the mean flipping rate constant (Figure 2) shows an Arrhenius dependence with an

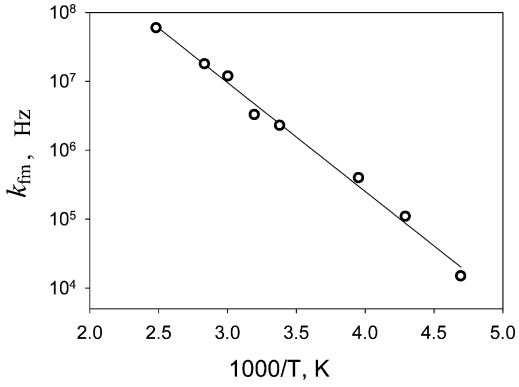

Figure 2. Arrhenius plot for the mean flipping rate constant k_{fm} in UiO-66.

activation barrier $E = 30 \pm 2$ kJ mol^{-1} and a preexponential factor of $k_{fm0} = (0.5 \pm 0.8) \times 10^{12}$ s^{-1}. The width of the flipping rate distribution σ covers more than two decades of possible flipping rates, and it hardly varies within the whole experimental temperature region.

The distribution of the flipping rates effectively separates all organic linkers into three categories: (i) those static on the ^{2}H NMR time scale, with $k_f < 10^3$ s^{-1}; (ii) the ones slowly mobile, with $10^3 < k_f < 10^6$ s^{-1}, and (iii) the fast flipping fragments with $k_f > 10^6$ s^{-1}. The evaluation of each species population is presented in Figure 3. As expected, the low-mobility linker population decreases with temperature rise, while the amount of fast flipping benzene rings increases progressively.

dx.doi.org/10.1021/jp3029193 | J. Phys. Chem. C 2012, 116, 12131−12136

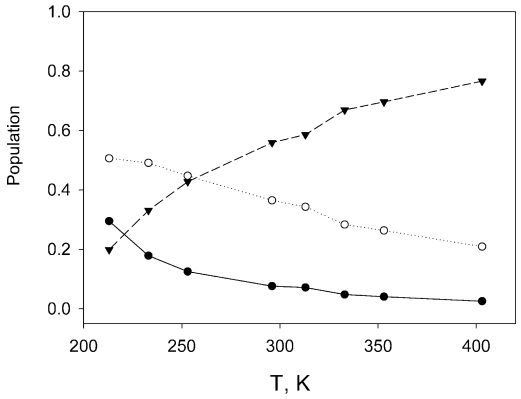

Figure 3. Relative population factors for the UiO-66 organic linkers having different mobilities: (●) *static* fragments with $k_f < 10^3$ s^{-1}, (○) *slow* flipping fragments with $10^3 < k_f < 10^6$ s^{-1}, (▼) *fast* flipping fragments with $k_f > 10^6$ s^{-1}.

The libration of the organic linkers appears to be notably large only above 333 K, with a librational amplitude growing steadily with temperature up to $\Delta\varphi/2 = 15°$.

3.2. Neutron Scattering. The temperature dependence of the elastic intensity scattered by UiO-66 is shown in Figure 4

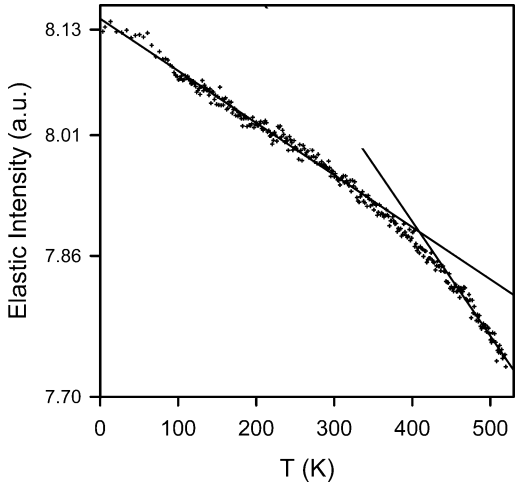

Figure 4. Elastic neutron intensity scattered by UiO-66 as a function of temperature.

on a logarithmic scale, and it corresponds to a sum over a Q range 0.19−1.6 Å^{-1}. The linear variation which is observed below ≈350 K can be attributed to the Debye−Waller factor, $\exp(-Q^2\langle u^2\rangle)$, where $\langle u^2\rangle$ is the mean square amplitude of the hydrogen atoms.

A change in slope in an elastic scan is typical of a transition in the sample. Since there is no structural phase transition for UiO-66, the different slope observed above ≈450 K indicates that the hydrogen atoms have access to an additional motion, i.e., the rotation of the benzene rings, which is fast enough to fit on the time scale of the experiment. This was checked by measuring QENS spectra at two temperatures, 300 and 510 K, situated below and above the "transition" observed around 400 K.

The spectra shown in Figure 5 correspond to a sum over a large number of detectors, to get reasonable statistics. As illustrated in Figure 5(a), the intensity was normalized at the

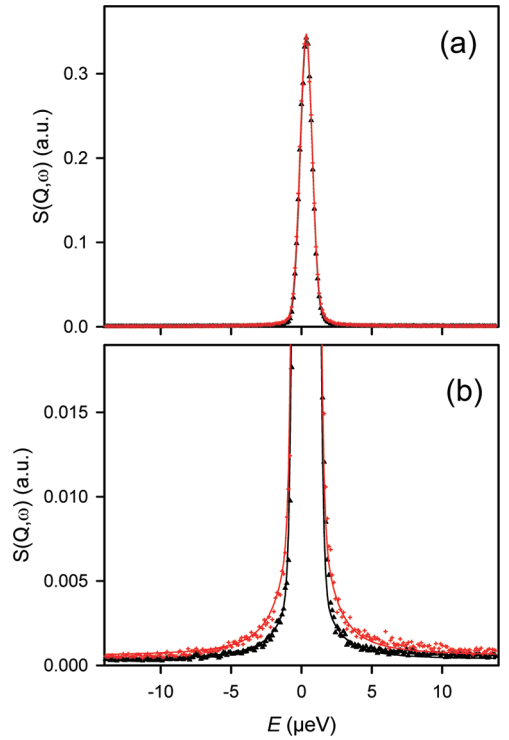

Figure 5. QENS spectra measured for UiO-66 at 300 K (▲) and at 510 K (red +). (a) and (b) correspond to the same data, but with different intensity scales.

maximum. The larger broadening obtained at 510 K is more evident in Figure 5(b), after enlarging the ordinate scale.

4. DISCUSSION

The QENS spectrum measured at 300 K corresponds to the instrumental resolution, which implies that the rotation of the benzene ring of the BDC linkers is slower than 10^{-8} s. Above 400 K, the rotational motion enters the time scale window accessible by the spectrometer, which indicates that a fraction of the benzene rings have a flipping rate larger than 10^8 Hz. This is in nice agreement with the ^{2}H NMR results (Figure 2). However, it is difficult to extract from Figure 5 the proportion of rotating rings because it corresponds to a sum over a large Q range, 0.19−1.6 Å^{-1}, the elastic intensity varying with Q.[32] Another reason is that this sum includes the contributions from Bragg peaks which cannot be resolved on this spectrometer. The fact that no Q-dependence of the fwhm could be obtained is less problematic for a rotational than for a translational motion since the broadening generally varies less with Q.

A more quantitative analysis is obtained from the ^{2}H NMR data. The activation energy derived from the temperature dependence of the mean flipping rate constant, 30 kJ mol^{-1}, is within the range typical for phenyl fragments dynamics in solid polymers,[33,34] but the activation barrier is considerably reduced in comparison with other porous metal−organic frameworks. In MOF-5, the activation energy for the π-flip rate constant is 47 kJ mol^{-1},[21] in MIL-47 is 45 kJ mol^{-1},[25] and in MIL-53 is 41 kJ mol^{-1}.[25] The comparison indicates that the benzene rings are notably more mobile in UiO-66. Indeed, this is the first time that the rotation of the benzene rings is measured in MOFs by QENS.

The observation of a distribution of flipping rates is a consequence of a structural disorder, an inhomogeneity present

dx.doi.org/10.1021/jp3029193 | J. Phys. Chem. C 2012, 116, 12131−12136

in the UiO-66 system that itself is not affected by the temperature change. To our knowledge, the presence of such heterogeneity in the framework mobility is unique for MOFs. This finding is supported by the recent UiO-66 structure investigation where it was found that randomly distributed structure defects, due to the absence of 1/12 of the BDC ligands in the starting material, do not affect the crystallinity of the whole crystal but create a small range local disorder in metal−oxygen bond lengths.[28] In such a case, the width of the flipping rate distribution can be used as a sensor to evaluate the UiO-66 structure defects distribution.

The amplitude of libration of the aromatic rings is relatively small, especially when compared with noncrystalline polymer systems.[35] However, it should be emphasized that in the other MOFs studied so far by ^{2}H NMR (MOF-5, MIL-47, and MIL-53) no sign of such librations was monitored.

For the free diameter of the triangular window of UiO-66, values in the range 5−7 Å are quoted,[9,10] but because of the rotation of the benzene rings, the pore opening must be temperature dependent. In a previous study of methane diffusion in UiO-66, a nonmonotonous evolution of the self-diffusion coefficient of CH_4 was observed at 230 K, with a maximum at intermediate loading.[11] Such behavior is typical of the concentration dependence obtained for narrow-window structures, so at this low temperature most of the windows are essentially closed (as shown in Figure 3, the majority of the linkers are either static or slowly rotating). On the other hand, bulky molecules like xylenes[10] or caffeine[36] can be adsorbed in the liquid phase above 300 K, where most of the linkers are fastly rotating. The adsorption and diffusion properties of this porous hybrid solid should therefore be affected by temperature. For separation applications using the UiO-66 series of solids, one may not only modify the linker but also consider other parameters such as the temperature.

■ ASSOCIATED CONTENT

Supporting Information

^{2}H NMR line shape simulation details. This material is available free of charge via the Internet at http://pubs.acs.org.

■ AUTHOR INFORMATION

Corresponding Author

*E-mail: herve.jobic@ircelyon.univ-lyon1.fr.

Notes

The authors declare no competing financial interest.

■ ACKNOWLEDGMENTS

We thank the Institut Laue-Langevin for neutron beam time. This work was supported by the Russian foundation for Basic Research (grants RFFI No. 12-03-00316 and No. 09-03-93113) and by the European Community's Seventh Framework Programme (FP7/2007-2013) under grant agreement no. 228862 (MACADEMIA project). The authors thank Dr. A. A. Gabrienko for preparation of the UiO-66 samples for the ^{2}H NMR experiments.

■ REFERENCES

(1) Bradshaw, D.; Claridge, J. B.; Cussen, E. J.; Prior, T. J.; Rosseinsky, M. J. *Acc. Chem. Res.* **2005**, *38*, 273.

(2) Li, H.; Eddaoudi, M.; O'Keeffe, M.; Yaghi, O. M. *Nature* **1999**, *402*, 276.

(3) Kitagawa, S.; Kitaura, R.; Noro, S. *Angew. Chem., Int. Ed.* **2004**, *43*, 2334.

(4) Férey, G.; Serre, C.; Devic, T.; Maurin, G.; Jobic, H.; Llewellyn, P. L.; De Weireld, G.; Vimont, A.; Daturi, M.; Chang, J. S. *Chem. Soc. Rev.* **2011**, *40*, 550.

(5) Férey, G. *Chem. Soc. Rev.* **2008**, *37*, 191.

(6) Farrusseng, D.; Aguado, S.; Pinel, C. *Angew. Chem., Int. Ed.* **2009**, *48*, 7502.

(7) Serre, C.; Millange, F.; Thouvenot, C.; Nogues, M.; Marsolier, G.; Louer, D.; Férey, G. *J. Am. Chem. Soc.* **2002**, *124*, 13519.

(8) Low, J. J.; Benin, A. I.; Jakubczak, P.; Abrahamian, J. F.; Faheem, S. A.; Willis, R. R. *J. Am. Chem. Soc.* **2009**, *131*, 15834.

(9) Cavka, J. H.; Jakobsen, S.; Olsbye, U.; Guillou, N.; Lamberti, C.; Bordiga, S.; Lillerud, K. P. *J. Am. Chem. Soc.* **2008**, *130*, 13850.

(10) Barcia, P. S.; Guimaraes, D.; Mendes, P. A. P.; Silva, J. A. C.; Guillerm, V.; Chevreau, H.; Serre, C.; Rodrigues, A. E. *Microporous Mesoporous Mater.* **2011**, *139*, 67.

(11) Yang, Q. Y.; Jobic, H.; Salles, F.; Kolokolov, D.; Guillerm, V.; Serre, C.; Maurin, G. *Chem.—Eur. J.* **2011**, *17*, 8882.

(12) Morris, W.; Taylor, R. E.; Dybowski, C.; Yaghi, O. M.; Garcia-Garibay, M. A. *J. Mol. Struct.* **2011**, *1004*, 94.

(13) Kim, M.; Garibay, S. J.; Cohen, S. M. *Inorg. Chem.* **2011**, *50*, 729.

(14) Yang, Q. Y.; Wiersum, A. D.; Llewellyn, P. L.; Guillerm, V.; Serred, C.; Maurin, G. *Chem. Commun.* **2011**, *47*, 9603.

(15) Zlotea, C.; Phanon, D.; Mazaj, M.; Heurtaux, D.; Guillerm, V.; Serre, C.; Horcajada, P.; Devic, T.; Magnier, E.; Cuevas, F.; Férey, G.; Llewellyn, P. L.; Latroche, M. *Dalton Trans.* **2011**, *40*, 4879.

(16) Vermoortele, F.; Ameloot, R.; Vimont, A.; Serre, C.; De Vos, D. *Chem. Commun.* **2011**, *47*, 1521.

(17) Kandiah, M.; Nilsen, M. H.; Usseglio, S.; Jakobsen, S.; Olsbye, U.; Tilset, M.; Larabi, C.; Quadrelli, E. A.; Bonino, F.; Lillerud, K. P. *Chem. Mater.* **2010**, *22*, 6632.

(18) Garibay, S. J.; Cohen, S. M. *Chem. Commun.* **2010**, *46*, 7700.

(19) Kandiah, M.; Usseglio, S.; Svelle, S.; Olsbye, U.; Lillerud, K. P.; Tilset, M. *J. Mater. Chem.* **2010**, *20*, 9848.

(20) Guillerm, V.; Gross, S.; Serre, C.; Devic, T.; Bauer, M.; Férey, G. *Chem. Commun.* **2010**, *46*, 767.

(21) Gould, S. L.; Tranchemontagne, D.; Yaghi, O. M.; Garcia-Garibay, M. A. *J. Am. Chem. Soc.* **2008**, *130*, 3246.

(22) Gonzalez, J.; Devi, R. N.; Tunstall, D. P.; Cox, P. A.; Wright, P. A. *Microporous Mesoporous Mater.* **2005**, *84*, 97.

(23) Mowat, J. P. S.; Miler, S. R.; Griffin, J. M.; Seymour, V. R.; Ashbrook, S. E.; Thompson, S. P.; Fairen-Jimenez, D.; Banu, A. M.; Duren, T.; Wright, P. A. *Inorg. Chem.* **2008**, *50*, 10844.

(24) Comotti, A.; Bracco, S.; Valsesia, P.; Beretta, M.; Sozzani, P. *Angew. Chem., Int. Ed.* **2010**, *49*, 1760.

(25) Kolokolov, D. I.; Jobic, H.; Stepanov, A. G.; Guillerm, V.; Devic, T.; Serre, C.; Férey, G. *Angew. Chem., Int. Ed.* **2010**, *49*, 4791.

(26) Winston, E. B.; Lowell, P. J.; Vacek, J.; Chocholoušová, J.; Michl, J.; Price, J. C. *Phys. Chem. Chem. Phys.* **2008**, *10*, 5188.

(27) Amirjalayer, S.; Schmid, R. *J. Phys. Chem. B* **2008**, *112*, 14980.

(28) Valenzano, L.; Civalleri, B.; Chavan, S.; Bordiga, S.; Nilsen, M. H.; Jakobsen, S.; Lillerud, K. P.; Lamberti, C. *Chem. Mater.* **2011**, *23*, 1700.

(29) Wiersum, A. D.; Soubeyrand-Lenoir, E.; Yang, Q.; Moulin, B.; Guillerm, V.; Ben Yahia, M.; Bourrelly, S.; Vimont, A.; Miller, S.; Vagner, C.; Daturi, M.; Clet, G.; Serre, C.; Maurin, G.; Llewellyn, P. L. *Chem. Asian J.* **2011**, *6*, 3270.

(30) Schmidt, C.; Kuhn, K. J.; Spiess, H. W. *Prog. Colloid Polym. Sci.* **1985**, *71*, 71.

(31) Schadt, R. J.; Cain, E. J.; English, A. D. *J. Phys. Chem.* **1993**, *97*, 8387.

(32) Jobic, H.; Bée, M.; Renouprez, A. *Surf. Sci.* **1984**, *140*, 307.

(33) Heaton, N. J.; Kothe, G. *J. Chem. Phys.* **1998**, *108*, 8199.

(34) Jelinski, L. W. In *High Resolution NMR Spectroscopy of Synthetic Polymers in Bulk (Methods and Stereochemical Analysis)*; Komoroski, R. A., Ed.; VCH Publishers: New York, 1986; Vol. 7, p 335.

(35) Wendoloski, J. J.; Gardner, K. H.; Hirschinger, J.; Miura, H.; English, A. D. *Science* **1990**, *247*, 431.

(36) Gaudin, C.; Cunha, D.; Ivanoff, E.; Horcajada, P.; Chevé, G.; Yasri, A.; Loget, O.; Serre, C.; Maurin, G. *Microporous Mesoporous Mater.* **2011**, DOI: 10.1016/j.micromeso.2011.06.011.